

Article

Fluorite Mineralization Related to Carbonatitic Magmatism in the Western Transbaikalia: Insights from Fluid Inclusions and Trace Element Composition

Anna A. Redina^{1,*}, Anna G. Doroshkevich^{1,2,*}, Ilya V. Veksler^{1,3} and Cora C. Wohlgemuth-Ueberwasser³

¹ Sobolev Institute of Geology and Mineralogy, Siberian Branch of the Russian Academy of Sciences, Akademika Koptiyuga Avenue 3, 630090 Novosibirsk, Russia; veksler@gfz-potsdam.de

² The Geological Institute Siberian Branch Russia Academy of Sciences, St. Sakhyanova 6a, 670047 Ulan-Ude, Russia

³ German Research Centre for Geosciences, GFZ, Telegrafenberg, 14473 Potsdam, Germany; cora.wohlgemuth-ueberwasser@gfz-potsdam.de

* Correspondence: redina@igm.nsc.ru (A.A.R.); doroshkevich@igm.nsc.ru (A.G.D.); Tel.: +7-913-373-0139 (A.A.R.)

Abstract: Fluorite mineralization associated with different types of magmatism is common in the Western Transbaikalia. This study deals with Arshan, Yuzhnoe, and Ulan-Ude fluorite occurrences, which are the most significant examples of carbonatite-related fluorite mineralization in the region. The present paper focused on new fluorite geochemistry and fluid inclusion data, is aimed at revealing conditions of the fluorite mineralization formation, highlighting its genetic relationship with magmatism, compared to other deposits of this type. All the three locations belong to the Late Mesozoic Central Asian carbonatite province. Fluorites here are characterized by high rare earth elements (REE), Sr, and elevated La/Yb values. Fluid inclusions data imply that the formation of fluorite mineralization is a long process extending from late magmatic to the hydrothermal stage. Early fluorite crystallized from sulfate-carbonate orthomagmatic fluids at temperatures up to 500 °C. True hydrothermal fluorite was formed from the same fluids that were probably mixed with meteoric waters, which caused the temperature to drop to below 420 °C and led to an increase in the chloride component. The REE compositions of fluorite from the studied locations are similar to compositions of REE-rich fluorites from carbonatite-related deposits around the world.

Keywords: REE fluorite; carbonatitic magmatism; fluorite geochemistry; fluid inclusion study; Central Asian Orogenic Belt



Citation: Redina, A.A.; Doroshkevich, A.G.; Veksler, I.V.; Wohlgemuth-Ueberwasser, C.C. Fluorite Mineralization Related to Carbonatitic Magmatism in the Western Transbaikalia: Insights from Fluid Inclusions and Trace Element Composition. *Minerals* **2021**, *11*, 1183. <https://doi.org/10.3390/min11111183>

Academic Editor: Alexander R Cruden

Received: 19 August 2021

Accepted: 23 October 2021

Published: 26 October 2021

Publisher's Note: MDPI stays neutral with regard to jurisdictional claims in published maps and institutional affiliations.



Copyright: © 2021 by the authors. Licensee MDPI, Basel, Switzerland. This article is an open access article distributed under the terms and conditions of the Creative Commons Attribution (CC BY) license (<https://creativecommons.org/licenses/by/4.0/>).

1. Introduction

Carbonatite melts generally have anomalously high contents of F, rare earth elements (REE), Sr, P, U and other incompatible lithophile elements. One of the most common minerals in carbonatite-related REE deposits worldwide is fluorite. Fluorite mineralization has been reported to form both at the magmatic (Mato Preto) [1] and the hydrothermal stages (Amba Dongar, Songwe Hill) [2,3]. In some cases, magmatic and hydrothermal fluorite occurs within the same deposit (e.g., Bayan Obo, Mushgai-Khudag) [4–7]. Fluorine, together with chlorine and sulfate, is an important ligand that controls the transport and deposition of REE [8]. That is why trace element composition of fluorite and information obtained from studies of fluid inclusions in this mineral provide valuable insights for sources of fluid (e.g., magmatic versus formation waters), fluid composition, the deposition conditions, and make inferences about the ore potential of individual deposits.

In the Western Transbaikalia, fluorite occurrences are ubiquitous and belong to the Central Asian fluorite-bearing province, which comprises various formations: low-temperature (50–200 °C) hydrothermal quartz-fluorite, fluorine-beryllium, molybdenum-tungsten, REE carbonatites [8,9]. Fluorite mineralization has been extensively studied in the region [9–15],

but most attention has been given to fluorite occurrences associated with granites. Here we present an overview and new information on the Arshan, Yuzhnoe and Ulan-Ude locations that are the key examples of fluorite mineralization related to the Late Mesozoic carbonatite-bearing magmatic complexes. We summarize previous studies that provided petrographic and mineralogical descriptions, and also age determinations for these occurrences [16–18]. In addition, we reviewed the available information on fluid inclusions. The data on fluid inclusions from the Arshan and Yuzhnoe occurrences have been limited to estimations of homogenization temperatures [16]. Fluid inclusions from the Ulan-Ude occurrence have been considered more broadly in a previous publication [18], which contains information about the homogenization temperatures and composition of the inclusions. Here we present first data on REE concentrations in fluorites, which help to establish a genetic link between fluorite mineralization and carbonatite magmatism, and conditions for the formation of fluorite mineralization. Investigations of rare earth elements have been widely used as a good indicator to describe the geochemical processes in fluorite mineralization. Rare earth elements' evaluation of ore-forming fluids in a wide range of fluorite deposits can provide insights into the evolution of fluids through various geological and geochemical processes involved. Also, we present Raman spectroscopy data on the composition of the gaseous phase in the inclusions, daughter mineral assemblages, revised data on the salinities and salt composition of aqueous solutions, and homogenization temperatures of the inclusions.

2. Geological Setting

The carbonatite-related fluorite occurrences are located within the Central part of the Sayan-Baikal fold belt [19,20]. The tectonic structure started to form in the late Caledonian era. Later, the structure of the Caledonides was almost completely reworked in the late Paleozoic by intraplate magmatism and in the Mesozoic by continental rifting. The last stage is associated with the formation of carbonatite-bearing complexes [17].

The tectonic control of the fluorite-bearing intrusive complexes is evidenced by their close proximity to deep faults that form the system of Gusino-Uda rift basins. According to Vorontsov et al. [21], the graben system and the late Mesozoic magmatism in the area belongs to the structures of the Tugnuisko-Khiloksky sector of the Western Transbaikalia rift region. The Arshan and Yuzhnoe occurrences are located within the Slyudinsky horst (Figure 1), which is composed mainly of Paleozoic gneisses, granites and schists. The horst is located in the northern part of a riftogenic depression filled with Cretaceous terrigenous-sedimentary rocks (conglomerates, sandstones with interlayers of gravels, mudstones and siltstones). The contact of Cretaceous deposits with the rocks of the Slyudinsky horst is tectonic.

Arshan carbonatites form three low sloping flow-like bodies preserved as erosional remnants with dimensions: 250 m × 75 m, 80 m × 50 m and 75 m × 50 m. Thickness of the bodies does not exceed 6 m. The age of the carbonatite was determined at 126 ± 16 Ma by the Rb-Sr method [22]. Arshan carbonatites host more than 30 minerals. The main minerals include calcite, bastnäsité, Ba and Sr sulfates, and fluorite (as much as 15%), which have been interpreted to form at the magmatic stage. The fluorite grains up to 2 mm in size are purple in color and have an isometric appearance. There are also veins and lenses composed of calcite, barite, fluorite, parisite and other minerals that are believed to have a hydrothermal origin. This fluorite occurs as relatively homogeneous and light-colored isometric grains up to 3 mm in size, which occupy 5–10% of the rock [23].

The Yuzhnoe occurrence is associated with early Cretaceous dikes of alkaline syenites, and more than 20 carbonatite bodies. Carbonatites and syenites were dated by the Rb-Sr method at 122 ± 4 Ma and at 130 ± 5 Ma respectively [22]. Carbonatites form breccia pipe-like bodies and veins cropping out over an area of about 2 km². The pipe-like bodies are up to 15–20 m in diameter and are represented by fine-grained rock of massive or weakly banded texture composed of calcite and minor fluorite (less than 5%). They contain numerous fragments of host rocks constituting up to 60–70% of the rock volume. Fluorite

forms colorless at the rims and intensely colored (vivid or dark purple) octahedral crystals (up to 0.1 mm in size) or their nest-like clusters in the central part. The veins of carbonatites range in thickness from 1 to 10 m and extend lengthwise to 100–300 m. Fine-grained groundmass of the veins is composed of calcite (80–90%), biotite, fluorite (up to 10%) and barite, and encloses phenocrysts of calcite and barite. Vein fluorite is colorless or slightly colored isometric grains and cubic crystals up to 2.5 mm in size, which are located in the carbonate matrix [24]. Detailed descriptions of the geological settings and mineral composition of the Arshan and Yuzhnoe occurrences have been published by Doroshkevich and Ripp [17,23,24].

The Ulan-Ude fluorite occurrence is located in the northern part of the Mesozoic riftogenic Ivolga-Ude depression (Figure 1). Late Cretaceous sediments lying on the eroded surface of the crystalline basement are widespread in this area and represented by sandstones, siltstones, shales and conglomerates. Gneisses, migmatites, granite gneisses, crystalline schists, and limestones compose the crystalline basement. Bastnäsitite-fluorite and calcite-bearing rocks are found along the Selenga coastline, in bedrock outcrops located in the center of Ulan-Ude city. The age of the fluorite-bearing rocks of the Ulan-Ude occurrence was established from phlogopite by the Ar-Ar method and is equal to 134.2 ± 2.6 Ma [18]. In composition, the rocks are close to bastnäsitite-fluorite aggregates in carbonatites of the Arshan occurrence. However, the fluorite content reaches 30–55%. Ulan-Ude fluorite forms phenocrysts up to 0.5–1.5 cm in size and grains (0.2–1.5 mm) in a carbonatite matrix. Bastnäsitite, phlogopite, and feldspar are associated minerals. The outer zone (<1 mm) of Ulan-Ude fluorite has a dark purple or black color. Ripp et al. [25] presented a comprehensive description of the Ulan-Ude occurrence.

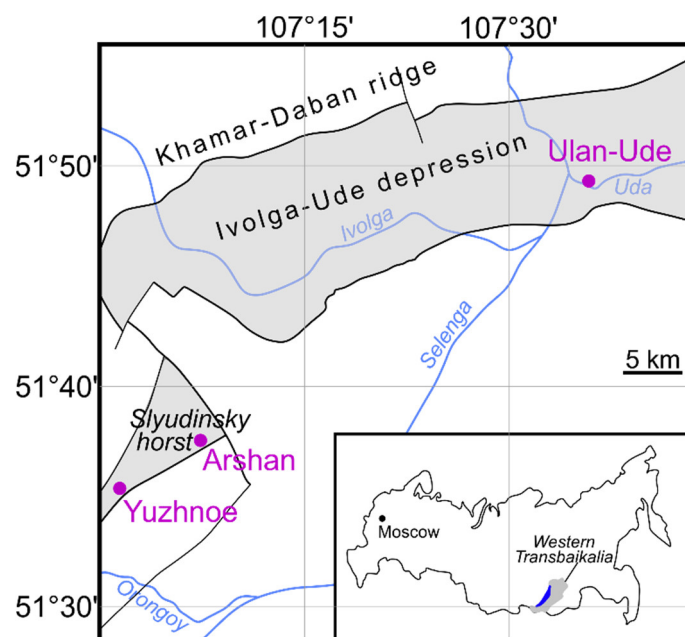


Figure 1. Tectonic position of the Arshan, Yuzhnoe, and Ulan-Ude occurrences [20].

3. Analytical Methods

Trace element data for fluorites were obtained by laser ablation ICP-MS analyses of individual fluorite grains mounted in epoxy resin. The analyses were carried out using Geolas Compex Pro 193 nm excimer laser coupled to a Thermo iCAP TQ mass spectrometer at GFZ Potsdam, Germany. Analytical conditions comprised a spot size of 24 μm , repetition rate of 8 Hz, and laser energy density of 5 J/cm². NIST SRM 610 was used as external standard. Calcium contents in fluorite determined by microprobe analysis were in the range of 60.9–67.3 wt.% CaO and they were used as an internal standard in calculations.

Detection limits: REE, Y 0.001 ppm; Sr, Zr, Nb, Ta 0.01 ppm; Ca 0.5 wt.%. Constructed REE plots are normalized to chondrite [26].

The fluid inclusion study was performed in the Sobolev Institute of Geology and Mineralogy, Siberian Branch of the Russian Academy of Sciences, Novosibirsk, Russia. For fluid inclusion studies, double-polished sections (0.3–0.5 mm) were prepared. Initial studies were carried out using an optical microscope Zeiss. The Roedder's criteria [27] were used to classify the fluid inclusions. Primary inclusions are observed as individual inclusions or in small groups within the core of crystals. Pseudo-secondary inclusions mark fissures within a single mineral grain. Secondary inclusions trace cracks across several grains or are in the recrystallization rims. Based on the phase composition at room temperature and phase transitions during heating and cooling, the fluid inclusions (FI) can be distinguished into three types: vapor-liquid double-phase (VL-type); multi-phase inclusions with vapor-liquid-solid phases (VLS-type); and multi-phase inclusions containing predominantly solid phases (CF-type). Microthermometric tests were carried out at Linkam THMSG-600, which allows the ability to perform real-time observations of phase transitions and temperature measurements in the temperature range from -196 to 600 °C. Microthermometric measurements were calibrated using synthetic fluid inclusion standards for the freezing points of pure CO_2 (-56.6 °C) and pure H_2O (0 °C), Reproducibility of calibrations are ± 0.6 °C for heating and ± 0.2 °C for freezing. Salt concentration in the inclusions was calculated from the ice melting temperature ($T_{m \text{ ice}}$) or solid phases melting temperature using calibration data from [28]. The salt composition of the solutions was determined from eutectic temperatures (T_e) [29]. Solid and gaseous phase composition was identified by Horiba Jobin Yvon LabRAM HR800 Raman microspectrometer (HORIBA France SAS) coupled with a CCD detector and an Olympus BX40 microscope, using a 532-nm Nd:YAG laser excitation at 50 mW, to a spectral resolution of $2\text{--}2.5 \text{ cm}^{-1}$. The monochromator was calibrated against the silica band (520.7 cm^{-1}). Selected integration time and number of accumulations equal 5 and 10 respectively. Mineral phases were identified using RRUFF database and CrystalSleuth software [30].

4. Results

4.1. Arshan

Fluorites of the Arshan occurrence can be divided into three groups according to mineral associations and the trace element composition (median, minimum and maximum values for each type of fluorite are given in Table 1). The first group is represented by fluorites related to carbonatites that form dissemination in calcite matrix. These fluorites have relatively flat chondrite-normalized REE spectra (Figure 2). They are characterized by depletion of light rare earth elements (LREE), as well as the absence of any obvious element anomalies. Fluorites of the first group have the highest REE and Sr contents. Total content of high field strength elements (HFSE) calculated as a sum of Zr, Nb and Ta concentrations (note that Hf and Ti values are usually below the detection limits) is at or below 0.5 ppm. Fluorites of the first group do not contain fluid inclusions.

Fluorite from veins and lenses constitutes the second and the third groups. The second group is characterized by chondrite-normalized REE spectra with a steep negative slope, a weak positive Eu anomaly, and an apparent Y negative anomaly. Total REE and Sr contents are the lowest for the Arshan fluorites. Total HFSE do not exceed 1 ppm. The third group shows moderate negatively sloped chondrite-normalized REE spectra with a weak Eu anomaly and a distinct positive Y anomaly. Strontium contents vary broadly. Total HFSE content is below 2 ppm.

Table 1. Trace element compositions (ppm) of fluorites from Arshan, Yuzhnoe and Ulan-Ude occurrences.

Occurrence		Arshan									Yuzhnoe						Ulan-Ude		
Group		1			2			3			1			2					
Value	med	min	max	med	min	max	med	min	max	med	min	max	med	min	max	med	min	max	
La	80.0	38.6	225	43.7	16.5	69.0	124	2.64	610	3240	111	9000	706	34.7	4880	10,000	108	83,000	
Ce	290	147	640	57.4	13.9	124	152	5.80	630	6670	293	17,000	1340	70.0	9400	17,100	152	134,000	
Pr	55.0	30.5	99.0	6.40	0.83	18.8	16.0	1.11	47.0	748	46.0	1720	173	14.6	1190	1570	15.9	11,500	
Nd	349	209	640	25.1	3.60	73.0	59.7	5.30	157	3010	177	6910	691	72.0	4620	4750	62.3	33,000	
Sm	116	71.3	180	2.86	0.34	9.40	9.06	1.46	21.5	330	28.2	776	93.5	9.10	562	371	12.4	1780	
Eu	41.6	27.9	67.0	0.89	0.31	2.84	4.46	0.81	18.2	71.0	8.50	172	21.5	3.93	110	87.1	4.87	289	
Gd	108	72.8	155	1.55	0.43	4.52	8.78	2.92	19.8	158	18.0	404	49.4	7.74	266	210	13.9	970	
Tb	12.5	7.90	22.0	0.17	0.03	0.48	1.15	0.39	2.19	10.3	1.47	25.5	3.54	0.66	17.0	16.9	2.14	51.2	
Dy	51.6	32.7	77.7	0.33	0.03	1.30	6.37	2.64	10.8	26.8	5.20	68.1	10.2	1.91	38.0	62.7	12.4	150	
Ho	7.29	5.01	11.1	0.12	0.01	0.35	1.29	0.67	2.49	3.57	0.82	8.27	1.41	0.36	4.90	10.4	2.53	25.2	
Er	13.4	8.80	22.0	0.17	0.02	0.44	3.33	1.70	6.60	7.61	1.54	16.8	3.03	0.71	10.5	26.5	7.90	61.9	
Tm	1.29	0.90	1.92	0.08	–	0.25	0.46	0.21	0.79	0.55	0.08	1.16	0.26	0.07	0.79	2.97	0.97	6.81	
Yb	6.31	4.31	10.1	0.12	–	0.38	2.37	1.42	3.76	2.99	0.29	6.31	1.34	0.28	3.79	19.3	6.30	43.8	
Lu	0.82	0.51	1.43	0.10	–	0.32	0.36	0.22	0.54	0.36	0.05	0.73	0.17	0.04	0.47	2.42	0.71	6.40	
Y	329	210	530	1.28	0.17	5.50	97.9	21.9	242	105	25	219	53.62	18.3	153	335	135	682	
Sr	4980	1230	48,200	974	474	2100	12,300	700	89,000	841	197	2350	4640	71.0	60,500	1960	239	12,800	
Zr	0.09	–	0.45	0.24	0.05	0.50	0.25	0.01	1.18	51.50	0.11	302.00	0.98	0.06	6.30	6.58	0.40	21.90	
Nb	0.09	–	0.27	0.18	0.04	0.38	0.82	0.05	1.59	0.27	0.04	0.64	0.09	–	0.50	1.85	0.12	6.20	
Ta	0.03	–	0.15	0.10	–	0.24	0.01	–	0.03	0.07	0.01	0.20	0.02	–	0.04	0.14	0.03	0.45	
La/Yb	13	6	38	2800	123	12,700	49	1	163	939	109	3082	416	15	2025	464	17	3897	
sum REE	1130	756	1890	139	38	305	389	29	1510	14,300	691	35,200	3100	251	21,100	34,300	402	265,000	
Eu*	1.11	0.86	1.47	1.39	0.99	2.40	1.22	0.75	2.61	0.99	0.85	1.12	1.10	0.84	1.39	1.07	0.65	1.36	
Y*	1.32	1.09	1.59	0.65	0.15	1.28	2.78	1.08	5.71	0.96	0.72	1.47	1.32	0.73	1.77	1.23	0.85	2.06	

Note: med—average value, min—minimum, max—maximum; “–”—below the detection limit; Eu*—Eu anomaly; Y*—Y anomaly.

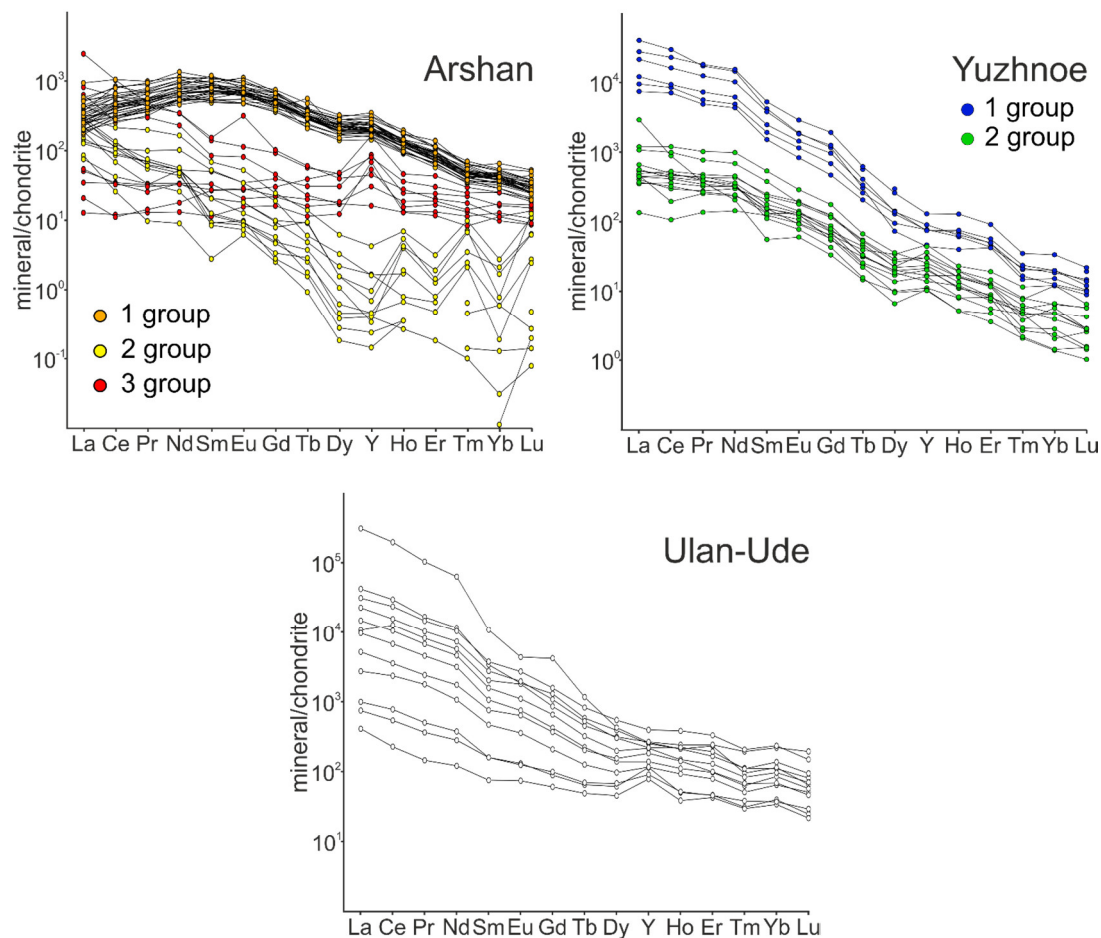


Figure 2. Chondrite-normalized REE + Y spectra of the fluorites [26].

Fluorite of the second and the third groups host multiphase crystal-fluid or CF-type (Figure 3a,b) and double-phase vapor-liquid (VL-type) inclusions (Figure 3f,g). Data on fluid inclusions are accumulated in Table 2. The study of primary CF and secondary VL inclusions allowed us to trace the evolution from initial orthomagmatic to hydrothermal mineralized fluid. Primary CF inclusions occur in small clusters in the central parts of the grains. They are isometric or elongated and up to 20 μm in size. Daughter mineral phases occupy 50–90 vol.% of the inclusions, and are represented by Na-Ca-Sr sulfates (sharp peaks at 995–1010 cm^{-1} , 1132 cm^{-1} , 1155–1160 cm^{-1} and triple peak at (610–)621–635–650 cm^{-1}) and Na-Sr carbonates (peak at 700–707 cm^{-1} and double peak at 1075–1078 cm^{-1}). Thermometric tests of the primary CF inclusions indicate homogenization temperatures (T_h) of 420–560 $^{\circ}\text{C}$ and salinities of 50–67 wt.% NaCl-equiv. Gaseous phase (~ 8 vol.%) consists of $\text{CO}_2 \pm \text{N}_2 \pm \text{H}_2$. Secondary VL inclusions trace cracks through several quartz grains and have irregular shapes and sizes of 2–8 μm . Gaseous phase occupies about 30–50 vol.% and is close to pure $\text{CO}_2 (\pm \text{N}_2)$. Ice melting temperatures for the secondary VL inclusions vary between -8 and -10 $^{\circ}\text{C}$. Homogenization temperatures and salinity values range between 90 and 150 $^{\circ}\text{C}$, and 11.7–13.9 wt.% NaCl-equiv. respectively. These results indicate that Arshan fluorites were formed from a homogeneous high-temperature sulfate-carbonate fluid (main cations Na, Ca, Sr). This was subsequently diluted by meteoric waters with a decrease in temperature and salinity.

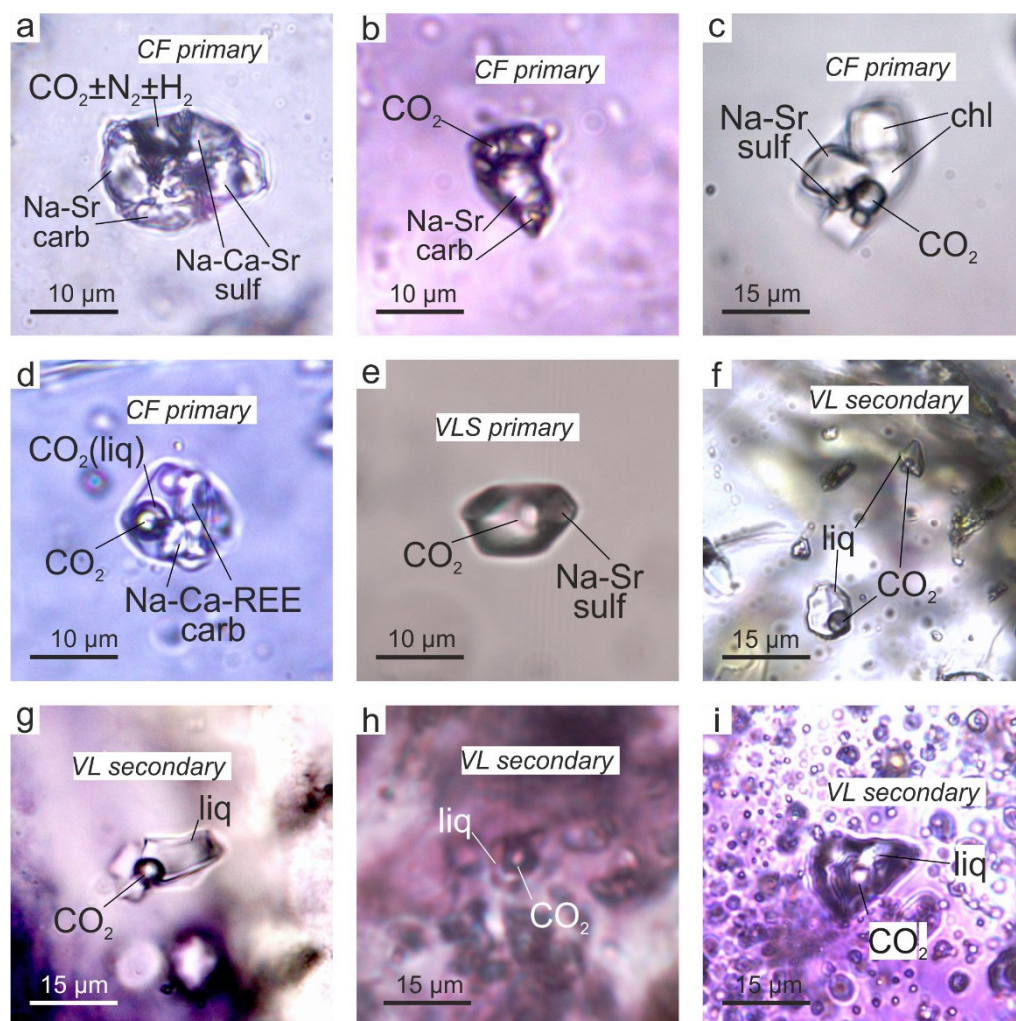


Figure 3. Primary inclusions in fluorite: (a,b) CF inclusions from Arshan occurrence; (c,d) CF inclusions from Ulan-Ude occurrence; (e) VLS inclusion from Yuzhnoe occurrence. Secondary inclusions in fluorite: (f,g) VL inclusions from Arshan occurrence; (h) VL inclusions from Yuzhnoe occurrence; (i) VL inclusions from Ulan-Ude occurrence. CO₂—carbon dioxide, liq—liquid phase, sulf—sulfates, carb—carbonates, chl—chlorides.

Table 2. Fluid inclusions in fluorites from Arshan, Yuzhnoe and Ulan-Ude occurrences.

Occurrence	Arshan		Yuzhnoe		Ulan-Ude	
FI type	CF, pr (12)	VL, s (14)	VLS, pr (10)	VL, s (15)	CF, pr (9)	VL, ps (7) VL, s (11)
T _{hom} , °C	420–560	90–150	360–470	110–165	440–520	135–250
Salinity, wt.% NaCl _{equiv.}	49.7–68.2	11.7–14	43.3–55.8		52–62.5	14.5–16
Gas phase	CO ₂ ± N ₂ ± H ₂	CO ₂	CO ₂ ± H ₂	CO ₂	CO ₂	CO ₂ ± N ₂ ± H ₂
Solid phase	Na ± Ca ± Sr sulfates and Na-Sr carbonates		Na-Sr sulfates, Na ± Ca carbonates and chlorides		Ca-Na-REE carbonates, Na-Sr sulfates and chlorides	

Note: FI—fluid inclusion, pr—primary, ps—pseudo-secondary, s—secondary. The number of studied inclusions is indicated in parentheses.

4.2. Yuzhnoe

By mineral associations, color, and trace element composition fluorites were divided in two groups. The first one is confined to areas of bastnäsite and albite accumulation in carbonatite. Here fluorite forms octahedral crystals (0.5–2 mm in size), which are colorless along the edges and dark purple in the center, and their clusters. Fluorites of this group have chondrite-normalized REE spectra with a strong negative slope (Figure 2). They have no Eu anomaly and a slight negative Y anomaly. Strontium concentrations are similar to

those of the second and the third groups at Arshan. The total HFSE contents vary broadly from 0.1 to 303 ppm (Table 1).

Fluorite crystals from fluorite-calcite matrix comprise the second group. This fluorite forms weakly purple or lilac isometric grains and cubic crystals 0.1–3 mm in size. In comparison to the first group, the second group is characterized by lower REE and Sr concentrations, a weakly positive Eu anomaly, and a clear positive Y anomaly. Total HFSE are up to 6 ppm. Fluorites from the second group of Yuzhnoe occurrence contain primary multi-phase VLS-type (vapor-liquid-solid) (Figure 3e) and secondary VL inclusions (Figure 3h). The VLS inclusions are negative crystal shape and 5–12 μm in size and localized randomly in fluorite's cores in groups. Daughter mineral assemblages (60–80 vol.%) of the VLS inclusions include Na-Sr sulfates (sharp peaks at 997–1000 cm^{-1} , 1152–1157 cm^{-1} and triple peak at 624–636–655 cm^{-1}), Na \pm Ca carbonates (sharp peaks at 712 cm^{-1} , 1075 cm^{-1} , 1086 cm^{-1}) and chlorides (no Raman spectra, optically isotropic cubic crystal) (Table 2). Liquid phase is a mixture of solution and liquid CO_2 . Gaseous phase (~10 vol.%) composition is $\text{CO}_2 \pm \text{H}_2$. The VLS inclusions yield T_h of 360–470 $^\circ\text{C}$ and salinities of 43–56 wt.% NaCl-equiv. The secondary VL inclusions are isometric up to 10 μm . Assemblages of the secondary FI occur in recrystallized rims. The gaseous phase (occupying ~40 vol.%) composed of CO_2 . The T_h fit into the interval 110–165 $^\circ\text{C}$. The fluorite of the Yuzhnoe occurrence was deposited from a homogeneous moderately hot chloride-sulfate-carbonate fluid. The main cations in the fluid are Na, Ca, Sr. During the development of the system, the fluid was diluted, and its temperature decreased.

Fluorite from the Ulan-Ude occurrence contains primary CF (Figure 3c,d) and pseudo-secondary and secondary VL inclusions (Figure 3i). The primary CF inclusions occur as negative crystal shape and up to 16 μm in size in unaltered parts of fluorite crystals. Daughter mineral assemblages of the CF inclusions include Ca-Na-REE carbonates (peaks at 686 cm^{-1} , 713 cm^{-1} , triple peak at 1082–1092–1099 cm^{-1}), Na-Sr sulfates (sharp peak at 992–998 cm^{-1} , double peak at 1132–1157 cm^{-1} and triple peak at 624–636–652 cm^{-1}) and chlorides (no Raman spectra, optically isotropic cubic crystal) (Table 2). Mineral phases occupy up to 80 vol. % of the inclusion. Carbon dioxide is occurred as gaseous and liquid phases (bubble up to 12 vol.%). The T_h and salinities values for the CF inclusions are in the range of 440–520 $^\circ\text{C}$ and 52–62 wt.% NaCl-equiv respectively. In some cases, it is possible to distinguish a boundary between liquid carbon dioxide and the gas bubble. Pseudo-secondary and secondary inclusions are irregular or isometric and up to 15 μm in size. They mark small cracks and occur in recrystallized rims of fluorite grains. Gaseous phase of the pseudo-secondary and secondary VL inclusions comprises $\text{CO}_2 \pm \text{N}_2 \pm \text{H}_2$ and occupies ~15 vol.%. The T_h are close to each other for pseudo-secondary and secondary inclusions and values are equal 135–250 $^\circ\text{C}$. The eutectic temperatures of the pseudo-secondary VL inclusions are between –19 and –15 $^\circ\text{C}$, implying a KCl-NaCl solution. The ice melting temperatures and salinities for these inclusions are –12 and –10.5 $^\circ\text{C}$ and 14.5–16 wt.% NaCl-equiv. respectively. Thus, the primary fluid inclusions from Ulan-Ude fluorite trapped homogeneous high-temperature chloride-sulfate-carbonate fluid (main cations are Ca, Na, REE, Sr). The later fluid contained in pseudo-secondary and secondary inclusions is moderately concentrated low-temperature chloride.

4.3. Ulan-Ude

Here fluorite forms phenocrysts up to 0.5–1.5 cm in size and smaller grains (from 0.2 to 3 mm) in carbonatite matrix. Bastnäsite, phlogopite, and feldspars are associating minerals. The outer zone (<1 mm) of the fluorite grains has a dark violet to black color, presumably due to radioactive irradiation. Fluorite mineralization from the Ulan-Ude occurrence is the richest in REE. The chondrite-normalized REE spectra are characterized by a negative slope flattening in the region of heavy REE, a lack of Eu anomaly, and a positive Y anomaly (Figure 2). The Sr content is similar to the average values in the other two occurrences that are described above. The HFSE content varies from 0.5 to 26 ppm (Table 1).

5. Discussion

5.1. Fluorite Geochemistry

The described features of the Arshan fluorites (Figure 4) suggest that fluorites of the first group are probably the earliest at the Arshan occurrence. They are characterized by the highest REE content and depletion in light REE, possibly due to co-crystallization with bastnäsite at the magmatic stage [31]. The second group fluorites apparently precede fluorites of the third group as the latter are distinguished by a lower (La/Yb)_n ratio and the appearance of a positive Y anomaly instead of a negative one, implying a greater degree of fractionation of the parental fluid [2,4,32]. A constant content of Sr, a gradual change in REE content and the ratio of light to heavy REE may indicate successive formation of the entire fluorite mineralization from a single source [33].

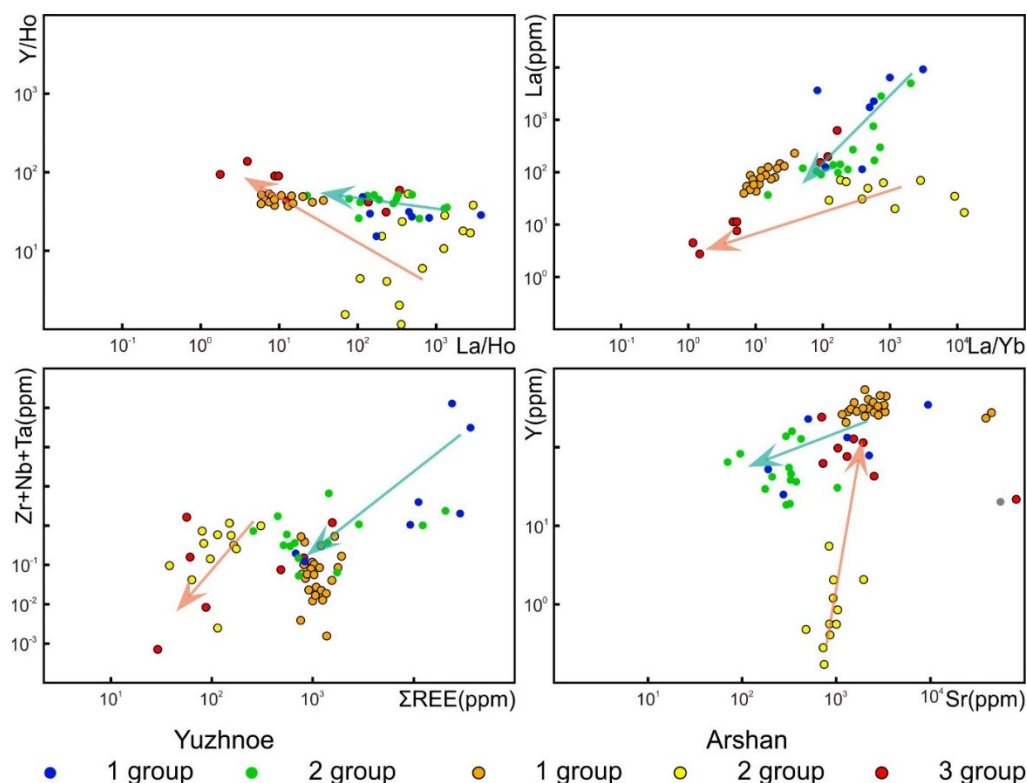


Figure 4. Groups of fluorites from Arshan and Yuzhnoe occurrences. Arrows indicate changes in the geochemical characteristics of fluorites from early to late for the Arshan and Yuzhnoye occurrences.

Fluorites of the Yuzhnoe occurrence are comparable to fluorites of the second and third groups from Arshan (Figure 4). Therefore, taking into account the above-listed criteria, we assume that the fluorites of the first group were formed earlier than the fluorites of the second one.

Fluorites of the Ulan-Ude occurrence belong to a single generation and are distinguished by the highest REE content and an apparent predominance of light REE.

The chondrite-normalized ratios and absolute REE concentrations in the fluorites allow to define rocks associated with fluorite mineralization. Generally, high REE concentrations, LREE enrichment and lack of a significant Eu anomaly are typical features of fluorites related to carbonatitic magmatism [34]. This confirms the direct genetic relationship between the studied fluorites and carbonatite magmatism.

The Möller Tb/Ca vs. Tb/La diagram [35] has been used to classify fluorites by mineral-forming processes, based on the features of REE. Our data for the Ulan-Ude, Yuzhnoe, and the first and second groups of the Arshan occurrence fall within the range of pegmatitic fluorite area (Figure 5). The fluorites of the Arshan third group lie below the pegmatitic/hydrothermal boundary in the area of hydrothermal fluorite, which confirms

our interpretation of them as the latest in formation. The Arshan occurrence is characterized by long-term multistage formation of fluorite mineralization. A similar situation was revealed in the Mushgai-Khudag complex, which contains several generations of fluorite from orthomagmatic to hydrothermal [7].

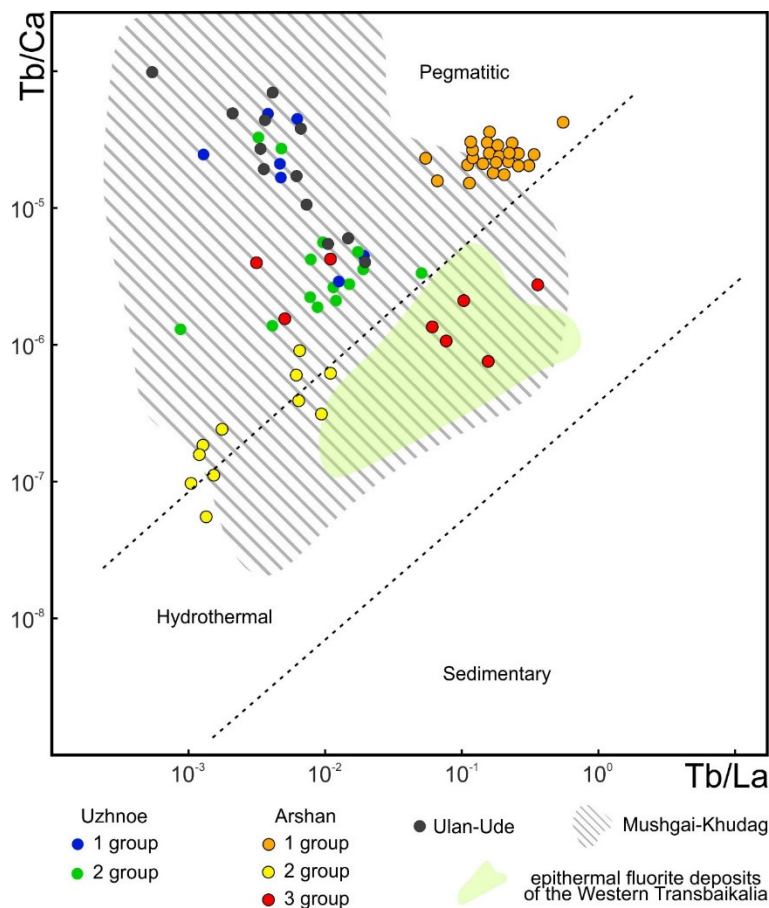


Figure 5. Tb/Ca vs. Tb/La diagram for the Transbaikalia fluorites (epithermal fluorite deposits of the Western Transbaikalia [10]; Mushgai-Khudag [7]).

5.2. Fluid Inclusions

Fluid inclusion studies of carbonatite-related fluorite mineralization worldwide have demonstrated wide ranges of homogenization temperatures and fluid salinities. The temperatures vary greatly from more than 500 to 100 °C. Salinities of fluids vary broadly from high to low; daughter minerals may be totally absent or may occupy more than 50 vol.% of an inclusion. Common daughter minerals are carbonates, sulfates, and chlorides of alkaline, alkaline-earth and rare-earth metals. Carbon dioxide is the most essential component of the vapor phase [2,4,7,36–41].

Our studies have revealed broad similarities between fluid inclusions at all the three fluorite occurrences. The fluid inclusions data demonstrate the involvement of sulfate-carbonate, hypersaline, high temperature orthomagmatic fluid at the start of fluorite formation. This fluid may belong to a trend originating directly from crystallizing carbonatitic magma. The fluid temperature and its salinity were apparently decreasing during the evolution of the magmatic-hydrothermal system. Fluid cooling probably was the main reason for the decreasing of REE, content in fluorites, especially strong for the light REE. The role of chloride ion in the hydrothermal mineralizing fluid apparently increased during the general cooling and chemical evolution. These features are common and characteristic for the Late Mesozoic fluorite mineralization in the Central Asian alkaline province

(for example, Mushugai-Khudag) and REE fluorite mineralization related to carbonatites worldwide.

5.3. Comparisons with Fluorites from Other Deposits

Carbonatites are generally enriched in REE (~2000 ppm), Nb (~1951 ppm), Zr (~1120 ppm), Mo, Y, Th and U, and impoverished in Ni, Cu, Cr, Au and other elements. This correlates quite well with the empirical data on carbonatite-related occurrences of the Western Transbaikalia and, in particular, fluorite mineralization.

The fluorites of the Ulan-Ude occurrence and the first group at Yuzhnoe (Figure 6) are probably products of the most extensive fractionation evidenced by the maximum REE contents and the highest (La/Yb)_n ratio. They are similar to orthomagmatic fluorites of carbonatite complexes [1]. Fluorites from Arshan and the second group fluorites of the Yuzhnoe occurrence are geochemically similar to hydrothermal fluorites from REE deposits associated with carbonatite magmatism [2–6,42]. The high strontium content and the REE enrichment of fluorites are also consistent with the settings of fluorite mineralization precipitated from carbonatitic fluids, which were dominated by Ca and carbonate ions, but also contained high concentration of F and REE, and generally resembled a carbothermal residue [31,43].

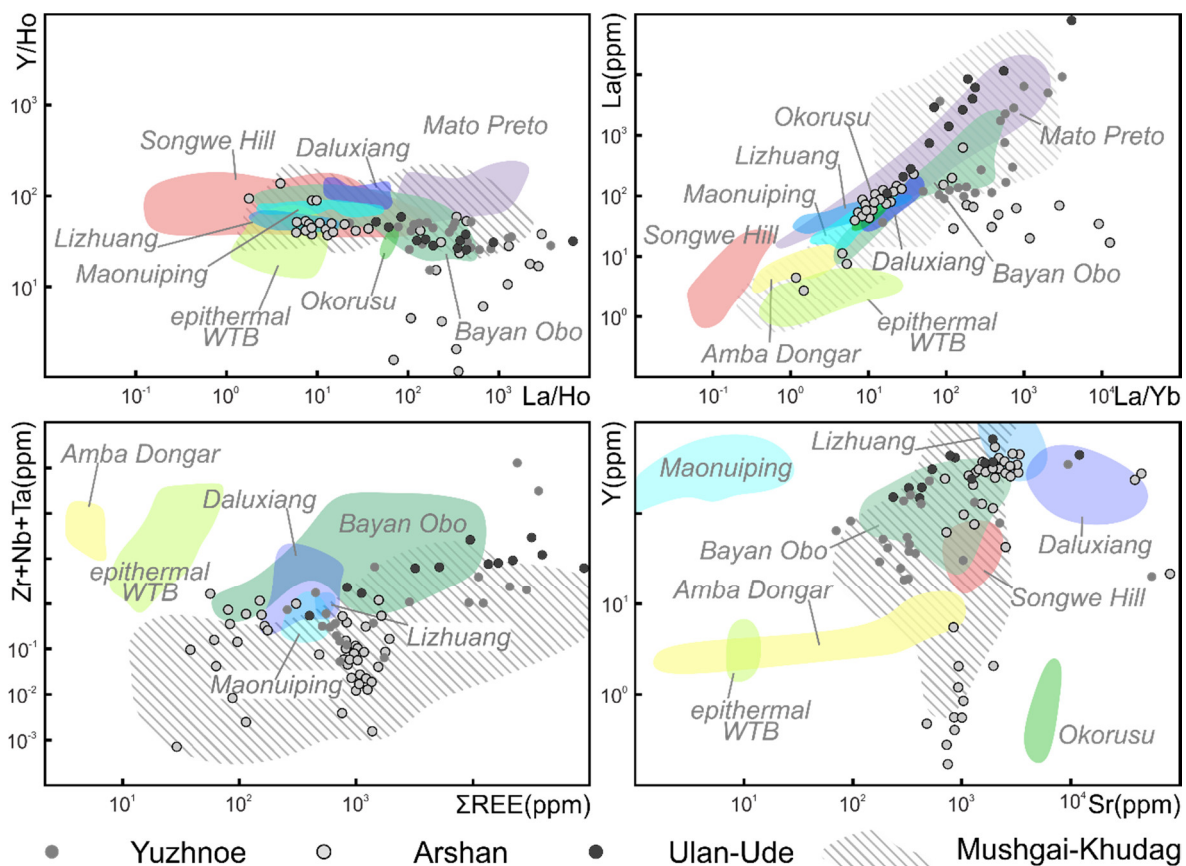


Figure 6. Plots of the Western Transbaikalia fluorites vs fluorites from REE deposits. (Amba Dongar [1]; Daluxiang, Lizhuang, Maonuiping, Bayan Obo [4–6]; Mato Preto [1]; Songwe Hill [3]; Okorusu [36]; epithermal WTB (epithermal fluorite deposits of the Western Transbaikalia) [10]; Mushgai-Khudag [7].

Our data compare well with key geochemical characteristics of fluorite mineralization genetically related to carbonatite magmatism and the largest REE deposits in the world (Figure 6). The fluorite mineralization studied here is clearly distinguished from late-stage, low temperature fluorite, e.g., at the Amba Dongar deposit or from the epithermal fluorite deposits of the Western Transbaikalia [2,10].

6. Conclusions

Fluorite mineralization related to carbonatite magmatism of the Central Asian carbonatite province was formed from highly concentrated orthomagmatic high temperature (400–500 °C) fluid of a sulfate-carbonate composition. The fluorite compositions are characterized by high contents of REE and Sr, and LREE predominance over HREE. Fluid inclusions data and the trace element compositions are typical for fluorite mineralization associated with carbonatites.

Author Contributions: Conceptualization, A.A.R. and A.G.D.; provision of study materials A.G.D.; data curation and validation A.G.D., I.V.V. and A.A.R.; writing—original draft A.A.R. and A.G.D.; investigations A.A.R. and C.C.W.-U.; writing—review and editing, A.A.R., I.V.V., C.C.W.-U. and A.G.D. All authors have read and agreed to the published version of the manuscript.

Funding: The LA-ICP-MS analyses were supported by the Russian Science Foundation, grant No. 19-17-00013.

Data Availability Statement: Not applicable.

Acknowledgments: The work was done on state assignment of IGM SB RAS (0330-2016-0002) and GIN SB RAS (No. AAAA-A21-121011390002-2).

Conflicts of Interest: The authors declare no conflict of interest.

References

- Santos, R.V.; Dardenne, M.A.; De Oliveira, C.G. Rare earth elements geochemistry of fluorite from the Mato Preto carbonatite complex, Southern Brazil. *Rev. Bras. Geociênc.* **1996**, *26*, 81–86. [[CrossRef](#)]
- Palmer, D.S.; Williams-Jones, A. Genesis of the Carbonatite-Hosted Fluorite Deposit at Amba Dongar, India: Evidence from Fluid Inclusions, Stable Isotopes, and Whole Rock-Mineral Geochemistry. *Econ. Geol.* **1996**, *91*, 934–950. [[CrossRef](#)]
- Broom-Fendley, S.; Brady, A.E.; Wall, F.; Gunn, G.; Dawes, W. REE minerals at the Songwe Hill carbonatite, Malawi: HREE-enrichment in late-stage apatite. *Ore Geol. Rev.* **2017**, *81*, 23–41. [[CrossRef](#)]
- Xu, C.; Taylor, R.N.; Li, W.; Kynicky, J.; Chakhmouradian, A.R.; Song, W. Comparison of fluorite geochemistry from REE deposits in the Panxi region and Bayan Obo, China. *J. Asian Earth Sci.* **2012**, *57*, 76–89. [[CrossRef](#)]
- Liu, S.; Fan, H.-R.; Groves, D.I.; Yang, K.-F.; Yang, Z.-F.; Wang, Q.-W. Multiphase carbonatite-related magmatic and metasomatic processes in the genesis of the ore-hosting dolomite in the giant Bayan Obo REE-Nb-Fe deposit. *Lithos* **2020**, *354–355*, 105359. [[CrossRef](#)]
- Liu, S.; Fan, H.R.; Yang, K.F.; Hu, F.F.; Wang, K.Y.; Chen, F.K.; Yang, Y.H.; Yang, Z.F.; Wang, Q.W. Mesoproterozoic and Paleozoic hydrothermal metasomatism in the giant Bayan Obo REE-Nb-Fe deposit: Constrains from trace elements and Sr-Nd isotope of fluorite and preliminary thermodynamic calculation. *Precambrian Res.* **2018**, *311*, 228–246. [[CrossRef](#)]
- Redina, A.; Nikolenko, A.; Doroshkevich, A.; Prokopyev, I.; Wohlgemuth-Ueberwasser, C.; Vladykin, N. Conditions for the crystallization of fluorite in the Mushgai-Khudag complex (Southern Mongolia): Evidence from trace element geochemistry and fluid inclusions. *Geochemistry* **2020**, *80*, 125666. [[CrossRef](#)]
- Migdisov, A.; Williams-Jones, A.E.; Brugger, J.; Caporuscio, F.A. Hydrothermal transport, deposition, and fractionation of the REE: Experimental data and thermodynamic calculations. *Chem. Geol.* **2016**, *439*, 13–42. [[CrossRef](#)]
- Bulnaev, K.B. *Fluorite Deposits of the Western Transbaikalia*; Nauka: Novosibirsk, Russia, 1976. (In Russian)
- Lastochkin, E.; Ripp, G.; Tsydenova, D.; Posokhov, V.; Murzintseva, A. Epithermal fluorite deposits of the Transbaikalia. *Russ. Geol. Geophys.* **2021**, *4*. (In Russian) [[CrossRef](#)]
- Bulnaev, K.B. Late Mesozoic volcanites and fluorite deposits of the Transbaikalia and Mongolia: Age and genesis relationship. *Tikhookeanskaya Geol.* **2003**, *22*, 103–110. (In Russian)
- Bulnaev, K.B. About the source of fluorine in epithermal fluorite deposits. *Tikhookeanskaya Geol.* **2004**, *23*, 113–115. (In Russian)
- Bulnaev, K.B. The Arshan carbonatite deposit—Possible source of bastnäsite ore. *Otechestvennaya Geol.* **2007**, *3*, 63–65. (In Russian)
- Burtseva, M.V. Hydrothermal mineralization in rare-earth carbonatites from Arshan deposit (Western Transbaikalia). *Izv. SB RANS. Geol. Poiski I Razved. Rudn. Mestorozhdenii* **2010**, *36*, 34–40. (In Russian)
- Lastochkin, E.I.; Ripp, G.S.; Tsydenova, D.S.; Posokhov, V.F.; Murzintseva, A.E. Results of isotopic study of epithermal fluorite deposits of Western Transbaikalia (source of matter and fluids). *Geol. Prospect. Explor. Miner. Depos.* **2018**, *41*, 41–53. (In Russian) [[CrossRef](#)]
- Vinokurov, S.F.; Golubev, V.N.; Krylova, T.L.; Prokof'ev, V.Y. REE and Fluid Inclusions in Zoned Fluorites from Eastern Transbaikalia: Distribution and Geochemical Significance. *Geochem. Int.* **2014**, *52*, 654–669. [[CrossRef](#)]
- Doroshkevich, A.G.; Ripp, G.S. Estimation of the conditions of formation of REE-carbonatites in western Transbaikalia. *Russ. Geol. Geophys.* **2004**, *45*, 492–500.

18. Ripp, G.S.; Izbrodin, I.A.; Lastochkin, E.I.; Rampilov, M.O.; Doroshkevich, A.G.; Chromova, E.A. A new type of rare metal mineralization in the Western Transbaikalia. *Otechestvennaya Geol.* **2018**, *3*, 9–21. (In Russian)
19. Petrov, O.; Leonov, Y.; Tingdong, L.; Tomurtogoo, O.; Hwang, J.Y. (Eds.) *Tectonic MAP of Central Asia and Adjacent Areas; M 1:2,500,000*; VSEGEI Cartographic Factory: Saint-Petersburg, Russia, 2008.
20. Platov, V.S.; Tereshenkov, V.G.; Savchenko, A.A.; Busuek, S.M.; Anosova, G.B.; Polyanskii, S.A. (Eds.) *State Geological Map of the Russian Federation; M. 1:200,000. Ser. Selenga. Sheet M-48-VI*; VSEGEI Cartographic Factory: Moscow, Russia, 2000.
21. Vorontsov, A.A.; Yarmolyuk, V.V.; Komaritsyna, T.Y. Late Mesozoic-Early Cenozoic rifting magmatism in the Uda sector of Western Transbaikalia. *Russ. Geol. Geophys.* **2016**, *57*, 723–744. [[CrossRef](#)]
22. Ripp, G.S.; Doroshkevich, A.G.; Posokhov, V.F. Age of carbonatite magmatism in Transbaikalia. *Petrology* **2009**, *17*, 73–89. [[CrossRef](#)]
23. Doroshkevich, A.G.; Ripp, G.S.; Viladkar, S.G.; Vladykin, N.V. The Arshan REE carbonatites, Southwestern Transbaikalia, Russia: Mineralogy, paragenesis and evolution. *Can. Miner.* **2008**, *46*, 807–823. [[CrossRef](#)]
24. Ripp, G.S.; Kobylkina, O.V.; Doroshkevich, A.G.; Sharakshinov, A.O. *Late Mesozoic Carbonatites of Western Transbaikalia*; BSC SB RAS: Ulan-Ude, Russia, 2000. (In Russian)
25. Ripp, G.S.; Prokopyev, I.R.; Izbrodin, I.A.; Lastochkin, E.I.; Rampilov, M.O.; Doroshkevich, A.G.; Redina, A.A.; Posokhov, V.F.; Savchenko, A.A.; Khromova, E.A. Bastnaesite and Fluorite Rocks of the Ulan-Ude Occurrence (Mineral Composition, Geochemical Characteristics, and Genesis Issues). *Russ. Geol. Geophys.* **2019**, *60*, 1407–1424. [[CrossRef](#)]
26. McDonough, W.F.; Sun, S.S. The composition of the Earth. *Chem. Geol.* **1995**, *120*, 223–253. [[CrossRef](#)]
27. Roedder, E. *Fluid Inclusions*; De Gruyter: Berlin, Germany; Boston, MA, USA, 1984.
28. Steele-MacInnis, M.; Lecumberri-Sanchez, P.; Bodnar, R.J. HokieFlincs_H₂O-NaCl: A Microsoft Excel spreadsheet for interpreting microthermometric data from fluid inclusions based on the PVTX properties of H₂O-NaCl. *Comput. Geosci.* **2012**, *49*, 334–337. [[CrossRef](#)]
29. Borisenko, A.S. *Analysis of the Salt Composition of Solutions of Gas-Liquid Inclusions in Minerals by Cryometric Method. Fluid Inclusions Study for the Search and Study of Ore Deposits*; Nedra: Moscow, Russia, 1982. (In Russian)
30. Lafuente, B.; Downs, R.T.; Yang, H.; Stone, N. The power of databases: The RRUFF project. In *Highlights in Mineralogical Crystallography*; Armbruster, T., Danisi, R.M., Eds.; W. De Gruyter: Berlin, Germany, 2015.
31. Mitchell, R.H. Carbonatites and carbonatites and carbonatites. *Can. Miner.* **2005**, *43*, 2049–2068. [[CrossRef](#)]
32. Gagnon, J.E.; Samson, I.M.; Fryer, B.J.; Williams-Jones, A.E. Compositional heterogeneity in fluorite and the genesis of fluorite deposits: Insights from LA-ICP-MS analysis. *Can. Miner.* **2003**, *41*, 365–382. [[CrossRef](#)]
33. Schönerberger, J.; Köhler, J.; Markl, G. REE systematics of fluorides, calcite and siderite in peralkaline plutonic rocks from the Gardar Province, South Greenland. *Chem. Geol.* **2008**, *247*, 16–35. [[CrossRef](#)]
34. Magotra, R.; Namga, S.; Singh, P.; Arora, N.; Srivastava, P.K. A New Classification Scheme of Fluorite Deposits. *Int. J. Geosci.* **2017**, *8*, 599–610. [[CrossRef](#)]
35. Möller, P.; Parekh, P.P.; Schneider, H.J. The application of Tb/Ca-Tb/La abundance ratios to problems of fluorite genesis. *Miner. Depos.* **1976**, *11*, 111–116. [[CrossRef](#)]
36. Bühn, B.; Rankin, A.H.; Schneider, J.; Dulski, P. The nature of orthomagmatic, carbonatitic fluids precipitating REE, Sr-rich fluorite: Fluid-inclusion evidence from the Okorusu fluorite deposit, Namibia. *Chem. Geol.* **2002**, *186*, 75–98. [[CrossRef](#)]
37. Kynicky, J.; Smith, M.P.; Song, W.; Chakhmouradian, A.R.; Xu, C.; Kopriva, A.; Galiova, M.V.; Brtnicky, M. The role of carbonate-fluoride melt immiscibility in shallow REE deposit evolution. *Geosci. Front.* **2019**, *10*, 527–537. [[CrossRef](#)]
38. Öztürk, H.; Altuncu, S.; Haniççi, N.; Kasapçı, C.; Goodenough, K.M. Rare earth element-bearing fluorite deposits of Turkey: An overview. *Ore Geol. Rev.* **2019**, *105*, 423–444. [[CrossRef](#)]
39. Rankin, A.H.; Ni, P.; Zhou, J. Fluid inclusion studies on carbonatite dyke and associated quartzite in Bayan Obo, Inner Mongolia, China. *Acta Petrol. Sin.* **2003**, *19*, 297–306.
40. Smith, M.P.; Campbell, L.S.; Kynicky, J. A review of the genesis of the world class Bayan Obo Fe-REE-Nb deposits, Inner Mongolia, China: Multistage processes and outstanding questions. *Ore Geol. Rev.* **2015**, *64*, 459–476. [[CrossRef](#)]
41. Walter, B.F.; Giebel, R.J.; Steele-MacInnis, M.; Marks, M.A.W.; Kolb, J.; Markl, G. Fluids associated with carbonatitic magmatism: A critical review and implications for carbonatite magma ascent. *Earth-Sci. Rev.* **2021**, *215*. [[CrossRef](#)]
42. Fan, H.-R.; Yang, K.-F.; Hu, F.-F.; Liu, S.; Wang, K.-Y. The giant Bayan Obo REE-Nb-Fe deposit, China: Controversy and ore genesis. *Geosci. Front.* **2016**, *7*, 335–344. [[CrossRef](#)]
43. Bühn, B.; Rankin, A.H. Composition of natural, volatile-rich Na–Ca–REE–Sr carbonatitic fluids trapped in fluid inclusions. *Geochim. Cosmochim. Acta* **1999**, *63*, 3781–3797. [[CrossRef](#)]